Potential Functions for Diffusive Motion in Carbon Molecular Sieves

3 AUTHORS, INCLUDING:

Robert G. Jenkins
University of Vermont

143 PUBLICATIONS **2,425** CITATIONS

On the water surface, the egg lecithin in all these structures is fully hydrated and in the liquid-crystalline phase.[8] The dehydration which takes place during the high-vacuum degassing that precedes the shadow-casting may account for some of these observations.

Electron microscopy has thus disclosed unusual structures in the collapsed film of egg lecithin. Studies of this type should ultimately shed light on some aspects of biomembrane structure.

(8) Reiss-Husson, F.; Luzzati, V. *Adv. Biol. Med. Phys.* **1967**, *11*, 87.

Potential Functions for Diffusive Motion in Carbon Molecular Sieves

M. B. Rao and R. G. Jenkins*

Department of Materials Science and Engineering, The Pennsylvania State University, University Park, Pennsylvania 16802

W. A. Steele

Department of Chemistry, The Pennsylvania State University, University Park, Pennsylvania 16802

Gas–solid interaction potentials are calculated for a number of simple gases within the micropores of carbon molecular sieves. Effects of nonspherical molecular shape and the periodically varying potential which produces barriers to surface diffusion are both explicitly included. The critical dimensions for the onset of activated diffusion in a slit-shaped pore are determined and compared with experiment for each gaseous molecule. Barriers for surface diffusion in the $\langle 10\bar{1}1 \rangle$ and $\langle 11\bar{2}1 \rangle$ crystallographic directions are estimated. The role of the energy barrier to entry into a micropore in determining diffusion rates is discussed, and it is shown that this becomes the critical factor when the pore size is smaller than the critical dimension for a given gas.

Introduction

Molecular sieve materials are used in large-scale industrial processes for gas separation. These materials have pores of molecular dimensions that give rise to selective adsorption. The selectivity is a result of the different rates of activated diffusion into the pore structure. It is believed that the diffusing molecule experiences a net repulsive interaction upon entering these very narrow pores and thus must pass over an energy barrier to gain admittance to the adsorption volume. The differences in magnitudes of these energy barriers for various species gives rise to different diffusion rates and thus causes separation.

A fundamentally important parameter in the study of molecular sieves for separation processes is the critical pore dimension below which diffusion for a particular species becomes activated. This pore dimension is defined to be that for which the minimum potential for a diffusing species in the pore is zero. Previous attempts at calculating this critical pore size from the interaction potentials have been limited to simple gases (He, Ar, Ne, Kr);[1] estimates of the critical pore dimensions for more complex molecules have not been considered. In this paper, the critical pore dimensions and the diffusion activation energies are calculated for a number of nonspherical molecules in carbon molecular sieves.

The micropores of porous carbon materials are generally considered to be slit shaped. Thus, kinetic measurements of the adsorption of organic solvents show that planar molecules have easier access to these pores than spherical molecules.[2] Furthermore, measurements of the heat of adsorption of various gases seem to agree with a slit shaped rather than cylindrical pore model.[3,4] Walker and co-workers[1] have calculated the interaction potential for noble gases passing between two parallel graphite basal planes and found that diffusion becomes activated when the spacing between the pore walls becomes less than the sum of the kinetic diameter of the diffusing species and 1.6 Å. They reasoned that this factor of 1.6 Å arises from the π-clouds emanating from the carbon basal plane; thus each basal plane contributes 0.8 Å. The difficulties in using this technique to estimate the critical pore dimension are 2-fold. First, the value for the thickness of the π-clouds of the basal planes need not be the same as that for nonnoble gases. Second, estimates of the kinetic diameter of nonspherical diffusing species obtained from the gas are generally not applicable to the calculation of the critical pore dimension. The kinetic diameter in the gas phase is proportional to the cube root of the effective volume of the molecule when it rotates freely in three dimensions, whereas diffusion of nonspherical molecules through narrow pores involves at least some loss of rotational freedom since it is likely that the molecule enters the pore along its minimum dimension. The kinetic diameter as determined from gas-phase data is, therefore, unsatisfac-

(1) Walker, P. L., Jr.; Austin, L. G.; Nandi, S. P. In "Chemistry and Physics of Carbon"; Marcel Dekker: New York, 1966; Vol. 2, pp 257–371.

(2) Dacey, J. R.; Thomas, D. G. *Trans. Faraday Soc.* **1954**, *50*, 740.
(3) Perret, A.; Stoeckli, F. *Helv. Chim. Acta* **1975**, *58*, 2318.
(4) Stoeckli, F. *Helv. Chim. Acta* **1974**, *57*, 2192.

tory. For example, if the Kihara potential is applied to CO_2 and N_2, the kinetic diameters obtained are 3.30 and 3.09 Å for CO_2 and N_2, respectively.[5] This would suggest that N_2 should diffuse more rapidly than CO_2 in a carbon molecular sieve. However, it has been shown experimentally that CO_2 can diffuse more rapidly than N_2 at temperatures below 300 K.[1]

Kinetic diameters for pore diffusion of a nonspherical diffusing species can be estimated from the minimum dimension of the molecule calculated from the van der Waals radii of the constituent atoms and the bond lengths. If r_0 is the minimum dimension of the molecule, one has

$$\sigma = 2^{1/6}r_0 \tag{1}$$

where σ is the kinetic diameter (eq 1 is easily derived from the Lennard–Jones potential equation). When this technique is applied to CO_2 and N_2, the minimum dimensions are estimated to be 3.35 and 3.00 Å, respectively. Again, this is contrary to experimental findings.

A more quantitative approach would be to model the interaction potential for diffusing species in the pore and then to use detailed results to determine critical pore dimensions. Such calculations are presented below.

Theory

Models for the interaction of rare gases with a graphitic solid whose surface is a basal plane have been discussed extensively in the literature and summarized in several monographs.[6,7] It is generally accepted that a reasonably accurate representation of the total gas–solid potential function, $u(\mathbf{r})$, for a spherical atom located at a position $\mathbf{r}$ relative to the solid can be obtained by summing pairwise atom–atom interactions over the entire solid. The atom–atom interactions are usually taken to be Lennard-Jones (12-6) functions with parameters given by applying the Lorentz–Berthelot combining rules to the gas–gas interaction parameters and to an effective C–C interaction function. If ϵ and σ are the well-depth and size parameters in the Lennard–Jones function, one has

$$u_{X-X}(\mathbf{r}) = 4\epsilon[(\sigma/\mathbf{r})^{12} - (\sigma/\mathbf{r})^6] \tag{2}$$

where X–X denotes the interaction between two X atoms (gas–gas or C–C, in this case), and

$$\epsilon_{X-C} = (\epsilon_{X-X}\epsilon_{C-C})^{1/2} \tag{3}$$

$$\sigma_{X-C} = (\sigma_{X-X} + \sigma_{C-C})/2 \tag{4}$$

Since the X–X parameters are taken from independent studies of bulk properties such as the second virial coefficient, one is left with only the C–C parameters as adjustable factors. Fits of adsorption data to theory for the range of rare gases plus requiring the ϵ_{C-C} and σ_{C-C} give reasonable values for interplanar separation and cohesive energy in graphite yield satisfactory values for these parameters.

The extension of these ideas to the interaction of simple polyatomic gases with graphitic adsorbents has also been attempted. In the particular case of N_2[8] it appears that a realistic potential is obtained. The calculations yield an adsorption energy that is a function of the position of the adsorbate molecule relative to a surface unit cell as well as z, its distance from the surface. We denote position in a plane parallel to the surface by the two-dimensional
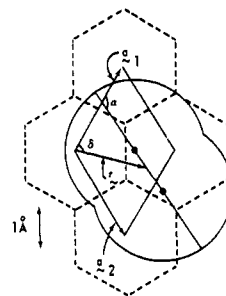
(5) Hirschfelder, J. O.; Curtiss, C. F.; Bird, R. B. "Molecular Theory of Gases and Liquids"; Wiley: New York, 1964.
(6) Young, D. M.; Crowell, A. D. "Physical Adsorption of Gases"; Butterworth: London, 1962.
(7) Steele, W. A. "The Interaction of Gases with Solid Surfaces"; Pergamon: London, 1974.
(8) Steele, W. A. *J. Phys. (Orsay, Fr)* 1977, *38*, Supp. C4, 61.

Figure 1. Schematic diagram of nitrogen molecule lying flat on graphite basal plane.

vector τ. For a linear molecule, the interaction also depends upon the orientation of the molecule relative to the surface, which will here be specified by defining β to be the angle between the molecular axis and the normal to the surface, and α, the in-plane orientation angle between the projection of the molecular axis onto the surface and a convenient surface lattice vector. Finally, the vector τ is written in polar coordinates with length τ and orientation γ to the surface lattice vector. These variables are the same as those used previously[8] and are shown pictorially in Figure 1.

The fact that the gas–solid potentials obtained from pairwise summations are quite complex functions had prevented their extensive use until it was noticed that important simplifications could be achieved by representing the interactions by a two-dimensional Fourier expansion (in τ). The proper symmetry of the surface lattice is readily and explicitly apparent because the expansion coefficients are multiples of the two-dimensional reciprocal vectors $\mathbf{b}_1$ and $\mathbf{b}_2$ for the surface. Thus, for a spherical atom, one writes

$$u(z,\tau) = w_{\mathbf{g}}(z) \cos (\mathbf{g}\cdot\tau) \tag{5}$$

where $\mathbf{g} = 2\pi(g_1\mathbf{b}_1 + g_2\mathbf{b}_2)$, with g_1 and g_2 equal to integers. For the Lennard–Jones atom–atom function, the coefficients $w_{\mathbf{g}}(z)$ are given by simple expressions that can be easily evaluated on a programmable hand calculator. An additional simplification can be introduced for graphitic substrates which is a consequence of the weak periodicity calculated for these materials. This allows one to truncate the Fourier series after the first set of three $\mathbf{g}$ vectors (of fixed length) and thus to write

$$u(z,\tau) = w_0(z) + w_1(gz)f(\tau) \tag{6}$$

where $f(\tau)$ is a sum of three cosine functions and g is the length of the smallest nonzero $\mathbf{g}$ vector for the graphite basal plane.

For a nonspherical molecule, the interaction energy can be modeled by a straightforward extension of the pairwise summation approach. One merely takes the polyatomic molecule to be composed of interaction sites located at the atomic positions, and extends the sums to include all sites in the molecule as well as all solid atoms. This site–site approach is known to work well in modeling bulk fluids and van der Waals solids, and it appears that it also gives a reasonable picture of the important features of the gas–solid interaction for molecules on graphite. Thus, for molecules one extends the Fourier representation for the basal plane by writing

$$u(\tau,\beta,\alpha,\gamma) = \sum_{i=1}^{n} w_0(z_i) + \sum_{i=1}^{n} w_1(gz_i)f_1(\tau,\gamma,\alpha) \tag{7}$$

where z_i is the distance between the ith site in the molecule and the surface and $f_1(\tau,\gamma,\alpha)$ is the sum of $f(\tau_i)$ over all sites in the molecule. The first term on the right-hand side of

Table I. Parameters for Adsorption Interaction Potential Equations

gas	$\epsilon_{g,i}/k$, K	$\sigma_{g,i}$, Å	bond length, Å
CO	C, 29 (14)	C, 2.785	1.12
	O, 83.1	O, 3.014	
CO_2	C, 29 (14)	C, 2.785	2.3
	O, 83.1	O, 3.014	
O_2	O, 58 (15)	O, 2.988	1.21
N_2	N, 34.32 (8)	N, 3.32	1.1
He	He, 15 (16)	He, 2.98	
Ar	Ar, 58 (16)	Ar, 3.38	
H_2[a]	H_2, 36 (17)	H_2, 3.04	

[a] Modeled as a spherical molecule.

eq 7 determines the gross changes in the interaction potential as each atom in the molecule moves away from the surface. The second term on the right-hand side of eq 7 determines the change in potential as the atom is moved within the unit cell. For linear molecules the position of each atom is determined relative to the position of the center of symmetry, z_c. For each atom,

$$w_0(z) = \sum_{m=0}^{\infty} \frac{4\pi\epsilon_{X-C}}{(a_s/q)} \left(\frac{1}{5} \frac{\sigma_{X-C}^{12}}{(z + md)^{10}} - \frac{1}{2} \frac{\sigma_{X-C}^6}{(z + md)^4} \right) \quad (8)$$

$$w_1(z) = \left(\frac{2\pi\epsilon_{X-C}}{a_s} \right) \left(\frac{\sigma_{X-C}^{12}g^5}{480z^5} K_5(gz) - \frac{\sigma_{X-C}^6 g^2}{z^2} K_2(gz) \right) \quad (9)$$

For a diatomic molecule,

$$f(\tau,\gamma,\alpha) = \sum_{l=1}^{2} \sum_{n=1}^{3} \cos\left[gt \sin\left(\gamma + \frac{2\pi n}{3} \right) + (-1)^l \frac{gL}{2} \sin\beta \sin\left(\alpha + \frac{2\pi n}{3} \right) \right] \quad (10)$$

where a_s is the unit cell area, q is the number of carbon atoms per unit surface cell, d is the distance between carbon planes, g is the reciprocal lattice vector, 2.95 Å^{-1}, L is the interatomic distance, and K_n is a modified Bessel function of the second kind.[9] The parameters ϵ_{X-C} and σ_{X-C} are given by the combining rules of eq 3 and 4; ϵ_{X-X} and σ_{X-X} have been determined for each atom in the adsorbing species by simulations or theoretical calculations of the bulk solid or liquid properties of the adsorbate; ϵ_{C-C} and σ_{C-C} are taken as 0.0564 kcal/mol and 3.4 Å, respectively.[7] Thus, the potentials are fully modeled and parameterized, at least for simple polyatomic adsorbates. In this paper, calculations have been performed on CO, CO_2, N_2, O_2, H_2, Ar, and He. The shape of H_2 was approximated as a sphere in the model since the H–H bond length is small; CO, CO_2, N_2, and O_2 were modeled as linear molecules. The pertinent constants used are given in Table I. The adsorption of these gases was first modeled considering only $w_0(z)$ terms. The w_1 terms of eq 7 were not considered on the grounds that the periodic terms are found to be very small at distances above the basal plane near the equilibrium distance.[7,8] Heats of adsorption at zero coverage were calculated from the potential functions and compared to experimental estimates as tests of the validity of the model for the molecules considered. The calculation was then extended to allow us to characterize the diffusion of these gases along the pore center line of a slit-shaped pore whose walls are composed of basal planes. In the calculations we have considered the w_0 and

Table II. Calculated and Experimental Heats of Adsorption on the Graphite Basal Plane

gas	ΔH_{cald}, kcal/mol	ΔH_{exptl}, kcal/mol (ref)
CO	2.40	2.58 (18)
H_2	1.05	0.90 (19,20)
CO_2	4.01	4.0 (19)
O_2	2.56	2.5 (19)
N_2	2.11	2.19 (8)
Ar	2.15	2.29 (19)
He	0.42	0.35 (19)

Table III. Summary of Calculated Critical Pore Dimensions

gas	slit width, Å
CO	5.41
H_2	5.48
CO_2	5.42
O_2	5.44
N_2	5.72
Ar	5.75
He	5.08

w_1 separately. First, changes in potential upon insertion of a molecule in the pore was determined by considering only the w_0 terms and superimposing the potential from each wall. The pore width at which the net potential energy change becomes zero was taken as the critical dimension. Finally, the energy barriers for diffusion in the $\langle 11\bar{2}1 \rangle$ and $\langle 10\bar{1}1 \rangle$ crystallographic directions were computed by calculating the w_1 terms within a pore with the critical pore dimension.

Results

The validity of the diffusion calculation is predicated on the ability to predict reasonable values of the heat of adsorption on the basal plane at zero surface coverage. Table II lists the calculated and experimentally estimated heats for the various species considered. It is evident that the model predicts the heat of adsorption fairly well for most species; the largest difference between the theoretical and experimental values is 0.2 kcal/mol for CO. Application of a quantum correction to the H_2 calculation should improve the agreement. These results provide confirmation that the model is a fair representation of the interaction potentials for these gases with the basal plane of carbon and indicates that this can be used to characterize the passage of these gases through pores.

For slit-shaped pores with parallel walls, it is easy to calculate the minimum pore width for unactivated diffusion. These widths were computed by summing the energies of interaction with each wall for a series of pore widths. The slit widths that give zero interaction potentials are given in Table III. The first observation is that the potentials calculated for the linear molecules strongly favor orientations parallel to the surface and these parallel orientations become more favorable as the wall separation decreases. Second, the order of effective molecular size for unactivated entrance into the pore is related to the critical pore dimensions and, thus, is He < CO, CO_2 < O_2 < H_2 < N_2 < Ar.

Discussion

When applied to Ar and He the present model gives results comparable to previous studies. Everett and Powl[10] provide two equations for the ratio of the interaction po-

(9) Abramowitz, M.; Stegun, I. A. "Handbook of Mathematical Tables"; National Bureau of Standards: Washington, DC, 1964.

(10) Everett, D. H.; Powl, J. C. *J. Chem. Soc. Faraday Trans. 1* **1976**, 72, 619.

tential along the pore center line to the potential minimum on a plane surface assuming either (9-3) or (10-4) potential functions. From their equations, the minimum pore widths for unactivated diffusion for Ar are 4.68 and 5.82 Å from the (9-3) and (10-4) models, respectively. The present model agrees with the (10-4) model of Everett and Powl rather than their (9-3) model. This observation is to be expected since the (10-4) function represents the surface-averaged energy with a given plane of carbon atoms, and near the minimum energy the sum is dominated by the leading term due to the outermost plane of solid atoms. These conclusions also apply to the He case, where Everett and Powl give minimum pore dimensions of 4.43 and 5.32 Å for (9-3) and (10-4) potentials, respectively. Although the (9-3) potential results agree with the results of Walker and co-workers,[1] the results from the present model again are in good agreement with the results obtained from the (10-4) potential function.

As discussed previously, a limitation of applying the method of Walker and co-workers[1] to the calculation of critical pore dimensions of nonspherical molecules is that gas-phase kinetic diameters are used which may not be characteristic of the critical pore size for entry. This method breaks down most obviously because the loss of rotational freedom during diffusion through narrow slits is not considered. As a result, experiments sometimes contradict theoretical calculations as with CO_2 and N_2. However, the present model gives critical pore dimensions that are commensurate with experiments for these species. Critical pore dimensions of CO_2 and N_2 are 5.42 and 5.72 Å, respectively. To the authors' knowledge, this is the first time that this anomaly between experiment and theory has been resolved.

The separation of O_2 and N_2 using carbon molecular sieves is currently generating a great deal of interest.[11] Experimental data on the adsorption rate of both O_2 and N_2 on given carbons show that O_2 can penetrate the pore structure more easily than N_2.[12,13] On the basis of estimates of the kinetic diameter either from the gas-phase models or determined from the minimum dimension, O_2 appears to be about 0.1–0.15 Å smaller than N_2. The present model shows that, indeed, O_2 is smaller than N_2 but by about 0.3 Å. The resulting larger difference in minimum pore size would also give rise to significant differences in diffusion activation energy. The repulsive interaction potential for the diffusion of N_2 through a pore of 5.44 Å in width is about 5.8 kcal/mol.

The model indicates that the critical pore dimension for H_2 is slightly larger than for CO_2, CO, or O_2. This suggests that the accessibility of pores to H_2 is somewhat smaller than to the other species, which is generally not found to be the case. However, the accessibility is also related to the energy barrier to diffusion which is dependent, in part, on the critical pore dimension. The energy barriers to diffusion will be now discussed further, but first it should be noted that the lack of a correction for quantum effects
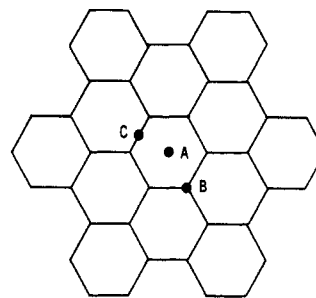
(11) Juntgen, H.; Knoblauch, K.; Harder, K. *Fuel* **1981**, *60*, 817.
(12) Koresh, J.; Soffer, A. *J. Chem. Soc. Faraday Trans. 1* **1980**, *76*, 2472.
(13) Nandi, S. P.; Walker, P. L., Jr. *Fuel*, **1975**, *54*, 169.
(14) Murthy, C. S.; O'shea, S. F.; McDonald, I. R. *Mol. Phys.* w1983, *50*, 531.
(15) Klein, M. J.; Levesque, D. D.; Weis, J. J. *Phys. Rev. B* **1980**, *21*, 5785.
(16) Steele, W. A. *J. Phys. Chem.* **1978**, *82*, 817.
(17) Schaeffer, J.; Watts, R. O. *Mol. Phys.* **1982**, *47*, 933.
(18) Morrison, J. A., Private communication.
(19) Avgul, N, N.; Kiselev, A. V. In "Chemistry and Physics of Carbon"; Marcel Dekker: New York, 1970f pp 1–124.
(20) Crowell, A. D.; Brown, J. S. *Surf. Sci.* **1982**, *123*, 296.

Figure 2. Center of symmetry positions for diffusion energy barrier calculations.

Table IV. Energy Barrier to Diffusion in the $\langle 10\bar{1}1 \rangle$ and $\langle 11\bar{2}1 \rangle$ Directions

| | energy barrier to diffusion, kcal/mol | | | |
| | $\langle 11\bar{2}1 \rangle$ | | $\langle 10\bar{1}1 \rangle$ | |
gas	max	min	max	min
CO	1.86	0.38	1.44	1.19
N_2	2.83	0.68	2.05	2.04
O_2	1.93	0.14	2.41	2.39
CO_2	9.19	1.16	3.82	3.06
H_2	1.65		0.41	
Ar	2.67		0.67	
He	0.93		0.23	

for the H_2 (and other molecules) calculation should yield larger calculated critical pore dimension.

Even though the criterion set forth for the critical dimension for entrance to a pore was that interaction potential be zero at the pore center line, it is necessary to remember that some energy barrier to diffusion does exist as the diffusing molecule moves from position to position over the surface due to the presence of discrete adsorption sites on the carbon basal planes. It is possible to calculate the energy barrier for diffusion for molecules traveling in various crystallographic directions through pores of any width by considering only the w_1 terms in the Fourier series of eq 7 and assuming a fixed distance from the surface so that the w_0 terms are constant. In this way, diffusional energy barriers for each species traveling in the $\langle 10\bar{1}1 \rangle$ and $\langle 11\bar{2}1 \rangle$ directions were computed. Molecules were placed on the pore center line in pores having the critical pore widths for diffusion calculated previously. The energy barrier for diffusion in the $\langle 10\bar{1}1 \rangle$ direction was taken as the difference in the interaction potential when the molecule lies with its center of symmetry at positions A and B in Figure 2. Likewise, the energy barrier for diffusion in the $\langle 11\bar{2}1 \rangle$ direction is the difference in potential between positions A and C. Linear molecules have some rotational freedom in the basal plane, and thus the diffusion energy barrier will be dependent on the α-angle at each position. This angle was thus varied, and the maximum and minimum energy barriers for diffusion in each direction have been computed.

Table IV shows that a wide range of diffusion energy barriers can exist depending on the nature of the molecule and its orientation on the surface unit cell. The true energy barriers will probably lie intermediate to those shown in Table IV. It appears that for Ar, He, and H_2 the $\langle 10\bar{1}1 \rangle$ direction is the preferred diffusion direction. For the linear molecules the diffusion barriers can vary over such a large range that it is difficult to assign a preferred direction. Furthermore, the range of possible diffusion barriers for each species overlap making it difficult to assign an order for the ease of diffusion. However, some inferences about the limiting steps to diffusion can be made.

There are essentially two barriers for activated diffusion. These are depicted in Figure 3. The diffusing species will
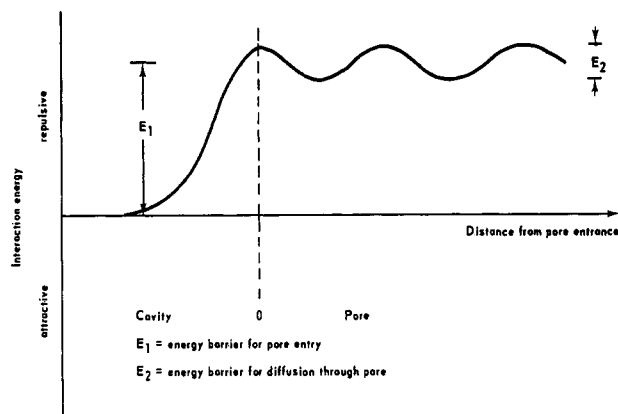
Figure 3. Energy barriers for diffusion through microporous carbon.

first have to enter the pore, probably from a large cavity. There will be an energy barrier, E_1, associated with this process, which can be estimated from eq 7. Once the molecule has entered the pore it must pass over an energy barrier E_2, in moving from position to position within the pore. The magnitude of this barrier depends, of course, on the specific crystallographic direction of diffusion. However, it is easy to show that the largest energy barrier for diffusion through pores smaller than the critical pore dimension occurs at the pore entrance. This indicates that the relative rates of diffusion for various species will often be dependent on the relative magnitude of this energy barrier. Thus, we examine the case of CO_2 and N_2 diffusing through a pore of width 5.42 Å. The mean value of the diffusional energy barrier within this pore (E_2) is ~1.5 kcal/mol for both CO_2 and N_2. This indicates that both species diffuse at about the same rate once they have entered the pore. The energy barrier for pore entry (E_1)

will be given by the w_0 terms of eq 7. The w_0 term for CO_2 diffusing through this pore is zero, however, for N_2 this term amounts to 5.8 kcal/mol. Thus, the limiting factor in N_2 diffusion appears to be the entry into this pore and not diffusion through it.

Hydrogen has been shown to have a slightly larger critical pore width than CO_2. The energy barrier for H_2 entering a 5.42-Å pore is 0.5 kcal/mol, compared to zero barrier for CO_2. The energy barrier for H_2 within the pore is 0.5 kcal/mol, which is significantly lower than the barrier within the pore for CO_2. Thus, even though it is slightly more difficult for H_2 to enter a 5.42-Å pore, it will diffuse more rapidly once inside the pore.

Although the critical pore width is defined to be representative of the energy barrier to pore entry, the relative magnitudes of the critical pore width for different species can be used only as a first approximation to estimate the separation efficiency in molecular sieve materials. The total rate of diffusion is dependent on the energy barrier for diffusion within the pores as well as the critical pore dimension and both factors must be taken into account when determining the accessibility of a species to the pore structure.

It should be emphasized that the model presented here is an idealized representation of the pore structure of carbon molecular sieves. The surfaces are assumed to be free of dislocations and chemisorbed surface complexes, are stationary, and are assumed to be perfectly parallel. Still, the model provides some insights into the relative rates of diffusion within carbon molecular sieves.

Subtractively Normalized Interfacial Fourier Transform Infrared Spectroscopy of Difluorobenzene Adsorbed at Polycrystalline Platinum Electrodes

Stanley Pons*

Department of Chemistry University of Utah, Salt Lake City, Utah 84112

Alan Bewick

Department of Chemistry, University of Southampton, Southampton, England S09 5NH

The subtractively normalized interfacial Fourier transform infrared spectra (SNIFTIRS) of the difluorobenzenes in perchloric acid solutions show that the species are absorbed flat at low concentrations of the substrate. In concentrated solutions, the packing changes to a tilted configuration. For these molecules there is no indication of vibrational coupling to the strong electrical field at the electrode surface and the vibrational spectra are as predicted by the standard surface selection rule.

Introduction

The study of adsorption of organic molecules at electrode surfaces is important to the areas of heterogeneous catalysis, corrosion, battery and fuel cell development, and electrosynthetic applications, to name a few. Conventional electrochemical methods can provide a great deal of information about surface excesses of adsorbed species and

strength of bonding of adsorbates at these surfaces. Recent work by Hubbard et al. has shown that it is possible to infer the molecular orientation of adsorbed organic species at platinum electrodes using an elegant differential thin-layer technique.[1] These workers have subsequently pro-

(1) Soriaga, M. P.; Hubbard, A. T. *J. Am. Chem. Soc.* **1982**, *104*, 3937.